HHS Public Access
Author manuscript
IEEE Trans Haptics. Author manuscript; available in PMC 2020 October 01.

Published in final edited form as:
IEEE Trans Haptics. 2019 ; 12(4): 563–570. doi:10.1109/TOH.2019.2914441.

Low Cost Haptic Simulation Using Material Fracture

David F. Pepley,
Nuclear and Mechanical Engineering Department, The Pennsylvania State University, University Park, PA 16802 USA

Yichun Tang,
The Pennsylvania State University, University Park, PA 16802 USA. He is now with Javan Engineering in Fort Washington, PA 19034

Sanjib D. Adhikary,
Anesthesiology and Perioperative Medicine Department, Penn State Health Milton S. Hershey Medical Center, Hershey, PA 17033 USA

Scarlett R. Miller,
School of Engineering Design, Technology, and Professional Programs, The Pennsylvania State University, University Park, PA 16802 USA

Jason Z. Moore
Nuclear and Mechanical Engineering Department, The Pennsylvania State University, University Park, PA 16802 USA

Abstract

Medical simulation training is widely used to effectively train for invasive medical procedures such peripheral nerve blocks. Traditionally, accurate haptic training relies on expensive cadavers, mannequins, or advanced haptic robots. Proposed herein is a novel concept for haptic training called the Low Cost Haptic Force Needle Insertion Simulator (LCNIS), which uses material fracture inside disposable cartridges to accurately replicate the force of inserting a needle into tissue. Cadaver and material fracture experiments are performed to develop and determine the accuracy of the LCNIS. The material testing showed that polycarbonate had the highest maximum needle puncture force of the materials tested, 9.85 N, and that fluorinated ethylene propylene had the lowest maximum puncture force, 0.84 N. The cadaver results showed that the error between the three peak forces in a cadaver and a cadaver mimicking cartridge was 1.00 N, 0.01 N, and 1.54 N. The standard deviation of these peaks was 0.60 N, 0.55 N, and 0.41 N. This novel method of haptic simulation can easily be adapted to recreate any type of force and therefore could be utilized to train for a wide variety of medical procedures.

Keywords

Needle Insertion; Force Feedback; Force Measurement; Training; Medical Simulation

---

(dfp5036@psu.edu).

I. Introduction

DELICATE hand motion control is a necessary skill for completing invasive medical procedures such as peripheral nerve blocks (PNB), epidural anesthesia, central venous catheterization, and laparoscopic procedures. These procedures involve the precise insertion of needles and controlled cutting punctures of tissue. For example, an ultrasound-guided PNB is a regional anesthesia procedure where an anesthetic drug is injected in close proximity to a peripheral nerve, such as the sciatic nerve using real-time image feedback from ultrasound [1]. PNB serves to interrupt pain signals allowing for effective pain relief or even completion of surgical procedures without the need for general anesthesia. It can also reduce the use of opioid based medications [2–4]. The effectiveness of the PNB depends on factors such as the precise placement of the local anesthetic around the target nerve without causing damage to the nerve or adjacent vital structures, and the amount of anesthetic injected. Failure to properly place the needle can result in a wide variety of adverse effects such as, neurological complications caused by nerve injury such as permanent neuropathy, transient neuropraxia hematoma due to vascular injury, ischemic injury caused by pressure and volume of the injected anesthetic, and in severe cases local anesthetic systemic toxicity can be caused by injection of anesthetic into the blood circulatory system [5–7]. Improved outcomes of ultrasound-guided PNB versus opioid based pain relief and general anesthesia have led to a significant increase in the use of ultrasound guided PNB over the past two decades, however there is currently no standard objective method for teaching ultrasound guided regional anesthesia procedures [8, 9].

Over the past 20 years, there has been a dramatic increase in the use of competency based, or mastery learning, medical education compared to the traditional Halstedian apprenticeship model of “see one, do one, teach one” as the primary method of resident training [10]. Competency based medical education is centered on achieving a set of core skill competencies and positive clinical outcomes as opposed to time-based training. This allows learners to progress at different rates and focus on their individual training needs. Recently this has been used in medical schools to train doctors before they start their training in a particular specialty as residents. Numerous studies have shown the highly effective nature of competency based education and the importance of a well-structured training program involving consistent high standards and objective measures of performance [11–13]. This paradigm shift in resident education along with other factors including ethical concerns about practicing on patients, increasing standards for operating room efficiency, restrictions on resident work hours, and decreased length of surgical clerkship has led to an increased use of simulators in resident training [14–17].

Simulators offer an effective way to train a wide variety of competencies and often allow residents to focus their training on a specific task. One of the most important competencies for an anesthesiologist to obtain is the ability to accurately place a needle with ultrasound guidance while causing minimal harm to surrounding tissue and structures [18, 19]. Evaluation of needle skills has been conducted using both direct observation by a trained expert and quantitative methods using computer based motion tracking [20, 21]. Through the use of motion tracking, it has been found that one of the key differentiators in needle insertion skills is in the difference in needle motion between experts and novices [20, 22–

25]. Experts have reduced movement, needle path length, and insertion time when compared to novices. Few anesthesia simulators for ultrasound guided procedures have been designed to address the training of these fine motor skills despite this understood difference between experts and novices. One possible method of improving fine motor skills is through the use of haptic training. Research has shown that early exposure to haptic training can enhance performance in surgical simulator training suggesting that haptic training can improve surgical skills [26].

This paper presents the development of the Low Cost Haptic Force Needle Insertion Simulator (LCNIS) which provides objective learning feedback, is inexpensive, and presents diverse patient training scenarios. Current medical training methods often use evaluation from a trained observer as their primary form of feedback. Unfortunately, this type of learning feedback can be subjective and observers have been found to suffer from “examiner burnout” over time [23, 27]. The LCNIS uses motion tracking to provide a more objective and real-time assessment of performance. State of the art medical training simulators such as central line manikins can cost from $400 to thousands of dollars, yet lack real time feedback, requiring a trained person to observe practice sessions to give feedback [28]. The LCNIS is inexpensive, around $119, making it an affordable alternative to commercial simulators. Finally, the LCNIS uses an innovative haptic cartridge to simulate needle insertion into a variety of human tissues. Traditional manikin simulators do not have this ability to train for a wide variety of patient scenarios. This leaves trainees unprepared for more difficult patients such as the obese or severely injured [29].

The following sections detail the design, development, and validation of the LCNIS. The materials and methods section will discuss the design of the LCNIS, as well as the cadaver study conducted to validate the forces in the haptic cartridge. Next, the results of the cadaver study and cartridge force validation will be presented. Finally, the discussions and conclusions section will evaluate the effectiveness of the haptic capabilities of the device, as well as future work to be conducted.

II. Materials and Methods

A. Design of the LCNIS

The design of the LCNIS, shown in Fig. 1, contains an innovative haptic cartridge to create a needle insertion force sensation for diverse patient scenarios. The LCNIS also contains an inertial measurement unit (IMU) and processor to measure movements and provide motion accuracy feedback. The syringe body of the LCNIS is 3D printed from acrylonitrile butadiene styrene (ABS) plastic and was designed to house the IMU, processor, and haptic cartridge. Precise guidance of the needle is achieved using a bronze bearing at the front of the syringe body. The needle used to puncture the haptic cartridge is a ground to a 30 degree round point and has a diameter of 1.60 mm.

The electronic processor and IMU component of the LCNIS are used for the real time measurement of the acceleration and angle of the device. The microcontroller used was a PJRC (Sherwood, OR) Teensy 3.2 which utilized I^2C serial communication with the IMU. The IMU was a SparkFun (Niwot, CO) MPU-9250 which contains an accelerometer to measure three dimensional acceleration and a gyroscope to measure changes in the angular velocity of the device. Equation (1) shows the complimentary filter used to calculate the real time angle of the device. Equation (2) is used to calculate the angle of the IMU from the measured 3-axis acceleration. Table 1 details the symbols used in (1) and (2).

$$\theta = 0.909 * (\theta_0 + \nu * dt) + (1 - 0.909) * \theta_x \tag{1}$$

$$\theta_x = \left(\frac{180}{\pi}\right) * \tan^{-1}\frac{a_x}{\sqrt{a_y{}^2 + a_z{}^2}} \tag{2}$$

The complimentary filter constant of 0.909 was calculated using a time constant of 0.1s and a device sample rate of 100Hz. The complimentary filter (1) is necessary to correct erroneous measurements due to natural drift in the gyroscope measurements and accelerometer measurements which are vulnerable to vibrations and noise. A complimentary filter is similar to a Kalman filter in that it is used to merge two different series of measurements into a single more accurate measurement. However, Kalman filters are computationally expensive, making a complimentary filter preferable during real-time calculations [30]. The calculated angles and acceleration are then transmitted to a connected PC using USB serial communication.

The haptic cartridge is a disposable cylinder filled with disks of material, as show in Fig. 2, that provide the force sensation of inserting a needle into tissue. To operate the LCNIS, the user presses the blunt tip of the LCNIS needle into a hard surface which causes the needle to retract into the haptic cartridge as shown in Fig. 2. There are two main components of needle insertion being simulated by the cartridge: large peaks in force that occur due to a build-up in force around the needle tip and eventual tissue fracture, and a gradual increase in force as the needle depth increases leading to increased friction [31]. These factors are the dominate features of needle insertion into soft tissue. To simulate the peaks in force, open slots along the body of the cartridge allow for disks of different haptic materials to be inserted at a variety of depths. Different disks of material provide varying levels of resisting force. For example, one disk may contain polycarbonate which provides very high needle puncture forces, whereas another disk may use polytetrafluoroethylene (PTFE) plastic film which provides low needle puncture forces. The increase in friction force over time is caused by materials such as a polyvinyl chloride (PVC) plastisol. When placed between the disks, this provides gradual increase in force as the depth of insertion increases. Varying thickness of simulated tissue layers can be achieved by varying the spacing of the material disks. The advantages of this cartridge include the ability to provide haptic feedback without complex and expensive computer simulation and easy to design cartridges to match a wide variety of needle insertion force profiles. Additionally, the outer cylinder of each cartridge lock the cartridge into four distinct insertion positions, permitting for four insertions per cartridge. To create haptic cartridges with force feedback that accurately simulates human tissue, experiments were conducted as detailed in the haptic cartridge force experiment section.

B. Cadaver Needle Force Experiment

Four experiments were performed to create haptic cartridges that provide realistic force feedback as seen in Table 2. Experiment 1 collected needle insertion forces from a cadaver. Experiment 2 determined the needle puncture forces of a variety of plastic materials for use in the haptic cartridge. Experiment 3 developed and validated an equation for predicting the force feedback from the haptic cartridges. Experiment 4 created a haptic cartridge to mimic needle forces measured during the cadaver experiment.

The cadaver insertions for Experiment 1 were conducted by an expert anesthesiologist with over 15 years of experience. Seven insertions were made into the thigh of a middle aged male cadaver using a Pajunk (Norcross, GA) SonoPlex Stim 21 Gauge 100 mm needle commonly used for PNB procedures. The thigh was chosen to simulate forces commonly associated with a sciatic PNB. Needle forces and position were measured using a previously developed force sensing needle [32]. This force sensing needle places an ATI Industrial Automation (Apex, NC) Nano17 6-axis force transducer between a fixed syringe handle and a standard leur lock syringe tip. For this experiment, the syringe measured axial needle forces. Position was obtained using a Northern Digital Inc. (Waterloo, Ontario, Canada) 3D Guidance TrakSTAR Model 80 electromagnetic position tracker. The anesthesiologist was directed to insert the needle at a constant velocity to obtain the needle insertion force versus the needle depth. The constant velocity was necessary in obtain a clear force profile based on needle depth.

C. Haptic Cartridge Force Experiments

Experiment 2 measured the needle puncture forces of six different plastic materials to determine the materials that would provide the force feedback in the haptic cartridge. The 30 degree, 1.60 mm diameter needle used in LCNIS was mounted to a computer controlled Dunkermotoren (Bonndorf, Germany) linear actuator which advanced the needle at a constant velocity of 5 mm/s and measured needle position as shown in Fig. 3. The needle cut through a variety of thin plastic materials, clamped between two disks, and attached to an ATI Industrial Automatic (Apex, NC) Gamma IP65 force transducer to measure needle forces versus the needle position. The plastic materials tested were 0.08 mm thick ABS, 0.13 mm thick ABS, 0.01 mm thick fluorinated ethylene propylene (FEP), 0.05 mm thick PTFE, 0.13 mm thick Polycarbonate, 0.10 mm thick Ultra-high-molecular-weight polyethylene (UHMW), and 12.7 mm thick PVC plastisol. These materials were chosen because due to their varying material strength properties. For example, the polycarbonate used has a tensile strength of 55.2 MPa while FEP has a tensile strength of only 20.7 MPa. Four needle insertions were conducted for each material.

Experiment 3 was conducted to validate an equation that would predict the needle forces measured from the haptic cartridge. The development of an accurate prediction equation is necessary for the development of future haptic cartridges. This equation will enable the quick development of new cartridges to match known force profiles. The LCNIS was mounted to the previously used linear actuator with the needle pushing into a metal plate attached to the Gamma 65IP force transducer at a rate of 5 mm/s as shown in Fig. 4. By pushing the blunt end of the needle into the metal plate, the 30 degree needle cutting tip is pressed through the haptic cartridge. This cutting force is then measured by the force transducer along with the position of the needle. Table 3 shows the materials used in the haptic cartridge, as well as the depths and thicknesses of each material in the cartridge. Between insertions, the cartridge was rotated 90 degrees to provide for a different entry point for each needle puncture. A total of four insertions were conducted into the cartridge. Experiment 4 used the same experimental procedure as Experiment 3 except the haptic cartridge used was designed to mimic the forces from the cadaver experiment. Eight insertions, four insertions each into two identical cartridges, were performed using this custom cadaver haptic syringe.

III. Results

The forces measured from one of the cadaver needle insertions in Experiment 1 are shown in Fig. 5. The results of the insertions showed a wide variety of different needle force profiles. The force profile shown in Fig. 5 was chosen to be mimicked by the LCNIS haptic cartridge because of its stable insertion velocity and minimal needle retraction. In the force profile, there is an early force peak of 8.56 N at a depth of 4.47 mm. This early peak occurs at the moment the needle breaks through the skin. The needle force then gradually increases over time to a maximum force of 15.5 N at a depth of 57.9 mm. While the force increases over time, there are a few sudden drops in force. This is typical of a needle insertion in biological tissue due to the lack of homogeneity of tissue and the periodic buildup and release of needle forces cutting into tissue [33].

For Experiment 2, the maximum needle forces and residual needle friction measured using the linear motor and thin plastic materials are shown in Table 4. Needle friction is defined as the average needle force measured after the needle tip has passed completely through the plastic material. The materials tested provide a wide variety of forces with the polycarbonate providing the strongest maximum puncture force at 9.85 N and the FEP providing the weakest maximum puncture force at 0.84 N. The different materials also had a low standard deviation of puncture force with the maximum standard deviation being 0.14 N in the polycarbonate and the lowest being 0.011 N in the 0.003” thick ABS. The PVC plastisol is a thicker and more flexible material than the other plastics tested. Because of this, the maximum insertion force occurs much deeper at 13.1 mm. The PVC plastisol was designed to be placed between thin disks of other materials in the cartridges.

Using the experimental data from Table 4, a piecewise linear equation was fit to approximate the needle cutting force and friction force of the PVC plastisol based on the thickness of the material. Using the experimental data from Experiment 2, Equation (3) was developed to predict forces from the LCNIS haptic cartridge based on the placement of the different plastics in the syringe and the depth of the insertion. The variables used in (3) are detailed in Table 5. For each peak in force in the piecewise equation, there are three main components. The first component involves the rise of forces while the needle is puncturing material as well as any previous residual needle friction. The second component is the rapid decrease in force after puncture occurs. This involves a rapid reduction in force from the peak insertion force to the final residual friction force in the material disk. Through testing, it was found that this reduction in force typically takes place over 0.5 mm. The third component of the equation is the residual friction from the material disk rubbing against the body of the needle.

$$F(x) = \begin{cases} \frac{F_{Pn}}{D_n - Z_n}(x - Z_n) + \sum_{i=1}^{n-1} f_i & \text{for } Z_n \le x \le D_n \\ \frac{f_n - F_{Pn}}{0.5}(x - D_n) + F_{Pn} + \sum_{i=1}^{n-1} f_i & \text{for } D_n < x \le D_n + 0.5 \\ \sum_{i=0}^{n} f_i & \text{for } D_n + 0.5 < x < Z_{n+1} \\ \vdots & \end{cases} \quad (3)$$

The results of Experiment 3, in Fig. 6, show the predicted forces using (3) for a haptic cartridge plotted against the actual forces recorded from insertions haptic cartridge Experiment 2. The five major peaks occur where the needle breaks through each of the 5 disks of material in the cartridge. A gradual increase in force also occurs between the first and second forces peaks due to the needle puncturing through the PVC plastisol. The error between the predicted force measurement and the average of the measured forces for each of the five force peaks were 0.27 N, −1.76 N, 0.13 N, −0.33 N, and −0.50 N. The standard deviation of each of the five force peaks were 0.04 N, 0.70 N, 0.47 N, 0.56 N, and 0.97 N showing consistency between insertions.

Experiment 4 used the data from the cadaver and plastic needle puncture experiments to create a custom cadaver haptic cartridge to mimic the forces of a PNB into the thigh of a cadaver. Table 6 shows the details of the materials used in the custom cadaver haptic cartridge. Fig. 7 shows the results of Experiment 4. The predicted needle insertion force is shown with the force measured from the cadaver mimicking haptic cartridge and the cadaver needle insertion experiment. Only one of the haptic cartridge insertions is shown in Fig. 7 for clarity. The error between the cadaver cartridge and the three main peaks was 0.01 N, 1.00 N, and 1.54 N. The error between the maximum force of the cartridge and the cadaver was 0.40 N. Again, there was consistency with the cartridge force peaks with the standard deviation of the three peaks being 0.60 N, 0.55 N, and 0.41 N. The standard deviation of the maximum force was 1.50 N.

IV. Discussion

The results of the cadaver experiment show that the initial puncture of the skin around the thigh provides a large amount of resisting force compared to the puncture of subcutaneous tissue. The skin puncture occurred at a depth of 4.47 mm, and the force transducer did not measure a force of this magnitude again until the needle reached a depth of 39 mm. This large skin puncture force is typical of needle punctures and poses one of the greatest challenges in accurately positioning a PNB needle [32]. Additional peaks in force occur throughout the insertion. During a needle insertion, an anesthesiologist should insert the needle at a controlled rate to prevent overshooting the target position or unintentionally harming nearby anatomical structures.

The results from the thin plastic material testing, Experiment 2, show a wide variety of needle puncture forces depending on the material. This variety makes these materials ideal for use in the LCNIS haptic cartridge as it allows for diverse haptic cartridges to be developed. Testing showed that using (3) in conjunction with the thin plastic material puncture data enables the accurate prediction of forces obtained from the haptic cartridges. The cartridge was also shown to be consistent for all four insertions into the material with insertion forces remaining within 1 N of each other between insertions. This consistency aided by the precision bearing placed at the front of the syringe accurately guiding the needle through 4 distinct puncture locations on the disks of materials as seen in Fig. 8. Through various testing, it was found that it is important for the plastic films in the disks to resist tearing between puncture holes. If tearing between holes occurs, the puncture force will not be accurately predicted.

The final validation testing, Experiment 4, showed that the custom cadaver haptic cartridge was able to successfully emulate the forces experienced during a needle insertion into a cadaver thigh. For this experiment, two identical cartridges were made. The low standard deviation of the force measurement results show that the cartridges can provide reliable repeatable force feedback. This repeatability is vital to the consistency of the system. The PVC plastisol placed between disks of other plastic materials enabled the cartridge to effectively emulate the gradual, continuous increase in force during a needle insertion. The third force peak in the custom cadaver cartridge was slightly larger than predicted. This is possibly due to the PVC plastisol pressing tightly into the PTFE disk. This may have negated the decrease in force that would be normally expected to occur when the needle tip exits the PVC since the tip immediately began pressing into the PTFE.

The LCNIS achieved its goal of being able to accurately simulate tissue forces. Equation (3) enables the accurate prediction of needle cartridge forces. Using (3) and the data from Experiment 2, all that would be required to create cartridges mimicking needle insertions into other parts of the body would be axial needle force insertion data based on depth such as that found in Fig. 5.

The LCNIS also achieved its goal of being low cost. The total cost of the electronic components is $47. Currently, the 3D printing cost of the syringe bodies and haptic cartridge cylinders is $58 and $14 respectively. Production for the LCNIS would use injection molding to significantly reduce this cost compared to 3D printing, with estimates for the cartridge cost being around $1. As currently designed, the device’s low cost cartridges would be disposed of after four insertions and replaced with new cartridges. The LCNIS provides an inexpensive alternative to robotic haptic training systems based on devices such as the 3D Systems (Rock Hill, SC) Geomagic Touch, which cost over $1000 before being integrated into a haptic training system.

V. Conclusions

The LCNIS is able to successfully emulate the forces experienced during a needle insertion at a fraction of the cost of traditional haptic training devices. The design of the LCNIS allows for easy exchange of its haptic cartridge and measurement of syringe movements.

Equations have also been developed that allow for the creation of custom haptic cartridges for use in the LCNIS. These cartridges are then able to recreate the forces experienced during a needle insertion into a variety of materials including needle insertions into cadaver tissue. Future work will include the creation of a graphical user interface for the LCNIS, and the development of a trainee performance assessment method utilizing the LCNIS's IMU capabilities to provide training of motor skills during needle insertion.

Acknowledgment

Research reported in this publication was supported by the National Heart, Lung, and Blood Institute of the National Institutes of Health under Award Number R01HL127316 and by the Penn State College of Engineering.

Biographies

David F. Pepley received his M.S. in Mechanical Engineering from Penn State University in 2017 and his B.S. in Mechanical Engineering from Grove City College in 2015. He is currently pursuing his Ph.D. in Mechanical Engineering at The Pennsylvania State University, University Park, PA, USA.

From 2015 to 2018 he was a Graduate Research Assistant in the Penn State Precision Medical Instrument Design Laboratory. His research interests include mechatronics, medical simulation and training, the interaction between medical instruments and tissue in the body.

Yichun Tang received his B.S. in Mechanical Engineering from The Pennsylvania State University in 2018. From 2017 to 2018 he served as an Undergraduate Research Assistant in the Penn State Precision Medical Instrument Design Laboratory and an Assistant Engineer at INFICON Instruments (Shangahi) Co., Ltd. He is currently a Design Engineer at Javan Engineering in Fort Washington, PA.

Sanjib Das Adhikary received his MD in Anesthesiology from Berhampur Medical University in India in 2002. He then did fellowships in Neuro-anesthesia from University of Toronto 2008 and Regional and Acute pain management from University of Western Ontario, Canada in 2009. He is currently a Professor of Anesthesiology and Perioperative Medicine, Orthopedics, and Rehabilitation and Division Director for regional anesthesia, acute pain medicine and orthopedics at Penn state College of Medicine. His research interest include ultrasound imaging education, anatomical correlation of ultrasound imaging to procedural skills and development of innovative ultrasound guided procedures for pain management.

Scarlett R. Miller received her B.S. and M.S. in Industrial Engineering from the University of Nebraska-Lincoln and her Ph.D. in Industrial Engineering from the University of Illinois at Urbana-Champaign in 2006, 2007, and 2011, respectively.

She is currently an Associate Professor of Engineering Design and Industrial Engineering at The Pennsylvania State University and director of the Bridging Research in Innovation Technology and Engineering Laboratory (britelab). Professor Miller's research interests include reducing error rates associated with medical procedure through the implementation of user-centered design practices.

Jason Z. Moore received his B.S., M.S., and Ph.D. degrees from the University of Michigan in 2006, 2007, and 2010, respectively.

He is currently an Associate Professor of Mechanical Engineering at The Pennsylvania State University and director of the Precision Medical Instrument Design Laboratory. Professor Moore's research interests include studying the interaction between medical instruments and tissue in the body and utilizing mechatronics to improve medical training and physical therapy devices.

References

[1]. Wright I, "Peripheral Nerve Blocks in the Outpatient Surgery Setting," AORN Journal, vol. 94, pp. 59–77, 2011. [PubMed: 21722772]

[2]. Hadzic A, Arliss J, Kerimoglu B, Karaca PE, Yufa M, Claudio RE, Vloka JD, Rosenquist R, Santos AC, and Thys DM, "A comparison of infraclavicular nerve block versus general anesthesia for hand and wrist day-case surgeries," Anesthesiology, vol. 101, pp. 127–132, 7 2004. [PubMed: 15220781]

[3]. Beaudoin FL, Haran JP, and Liebmann O, "A Comparison of Ultrasound-guided Three-in-one Femoral Nerve Block Versus Parenteral Opioids Alone for Analgesia in Emergency Department Patients With Hip Fractures: A Randomized Controlled Trial," Academic Emergency Medicine, vol. 20, pp. 584–591, 6 2013. [PubMed: 23758305]

[4]. Richman JM, Liu SS, Courpas G, Wong R, Rowlingson AJ, McGready J, Cohen SR, and Wu CL, "Does continuous peripheral nerve block provide superior pain control to opioids? A meta-analysis," Anesthesia and Analgesia, vol. 102, pp. 248–257, 1 2006. [PubMed: 16368838]

[5]. Liguori GA, "Complications of regional anesthesia - Nerve injury and peripheral neural blockade," Journal of Neurosurgical Anesthesiology, vol. 16, pp. 84–86, 1 2004. [PubMed: 14676576]

[6]. Jeng CL, Torrillo TM, and Rosenblatt MA, "Complications of peripheral nerve blocks," Br J Anaesth, vol. 105, pp. I97–I107, 12 2010. [PubMed: 21148659]

[7]. Brull R, McCartney CJL, Chan VWS, and El-Beheiry H, "Neurological complications after regional anesthesia: Contemporary estimates of risk," Anesthesia and Analgesia, vol. 104, pp. 965–974, 4 2007. [PubMed: 17377115]

[8]. Memtsoudis SG, Kuo C, Ma Y, Edwards A, Mazumdar M, and Liguori G, "Changes in Anesthesia-Related Factors in Ambulatory Knee and Shoulder Surgery United States 1996-2006," Regional Anesthesia and Pain Medicine, vol. 36, pp. 327–331, Jul-Aug 2011. [PubMed: 21490521]

[9]. Sites BD, Spence BC, Gallagher JD, Wiley CW, Bertrand ML, and Blike GT, "Characterizing novice behavior associated with learning ultrasound-guided peripheral regional anesthesia," Regional Anesthesia and Pain Medicine, vol. 32, pp. 107–115, Mar-Apr 2007. [PubMed: 17350520]

[10]. Carter BN, "The fruition of Halsted's concept of surgical training," Surgery, vol. 32, pp. 518–527. [PubMed: 12984268]

[11]. McGaghie WC, "Research opportunities in simulation-based medical education using deliberate practice," Acad Emerg Med, vol. 15, pp. 995–1001, 11 2008. [PubMed: 18811635]

[12]. Barsuk JH, Ahya SN, Cohen ER, McGaghie WC, and Wayne DB, "Mastery learning of temporary hemodialysis catheter insertion by nephrology fellows using simulation technology and deliberate practice," Am J Kidney Dis, vol. 54, pp. 70–6, 7 2009. [PubMed: 19376620]

[13]. Diederich E, Mahnken JD, Rigler SK, Williamson TL, Tarver S, and Sharpe MR, "The Effect of Model Fidelity on Learning Outcomes of a Simulation-Based Education Program for Central Venous Catheter Insertion," Simul Healthc, vol. 10, pp. 360–367, 12 2015. [PubMed: 26536341]

[14]. Frank JR, Snell LS, Cate OT, Holmboe ES, Carraccio C, Swing SR, Harris P, Glasgow NJ, Campbell C, Dath D, Harden RM, Iobst W, Long DM, Mungroo R, Richardson DL, Sherbino J, Silver I, Taber S, Talbot M, and Harris KA, "Competency-based medical education: theory to practice," Med Teach, vol. 32, pp. 638–45, 2010/08/01 2010. [PubMed: 20662574]

[15]. Harders M, Malangoni MA, Weight S, and Sidhu T, "Improving operating room efficiency through process redesign," Surgery, vol. 140, pp. 509–516, 2006/10/01/ 2006. [PubMed: 17011897]

[16]. Neumayer LA, Sachdeva AK, Hebert JC, and Lang NP, "Who should teach medical students surgery?," The American Journal of Surgery, vol. 173, pp. 218–219, 1997/03/01/ 1997. [PubMed: 9124630]

[17]. Choy I and Okrainec A, "Simulation in Surgery: Perfecting the Practice," Surgical Clinics of North America, vol. 90, pp. 457-+, 6 2010. [PubMed: 20497820]

[18]. Naik VN, Perlas A, Chandra DB, Chung DY, and Chan VWS, "An assessment tool for brachial plexus regional anesthesia performance: Establishing construct validity and reliability," Regional Anesthesia and Pain Medicine, vol. 32, pp. 41–45, Jan-Feb 2007. [PubMed: 17196491]

[19]. Friedman Z, Katznelson R, Devito I, Siddiqui M, and Chan V, "Objective assessment of manual skills and proficiency in performing epidural anesthesia - Video-assisted validation," Regional Anesthesia and Pain Medicine, vol. 31, pp. 304–310, Jul-Aug 2006. [PubMed: 16857550]

[20]. Chin KJ, Tse C, Chan V, Tan JS, Lupu CM, and Hayter M, "Hand Motion Analysis Using the Imperial College Surgical Assessment Device Validation of a Novel and Objective Performance Measure in Ultrasound-Guided Peripheral Nerve Blockade," Regional Anesthesia and Pain Medicine, vol. 36, pp. 213–219, May-Jun 2011. [PubMed: 21519307]

[21]. Slater RJ, Castanelli DJ, and Barrington MJ, "Learning and Teaching Motor Skills in Regional Anesthesia A Different Perspective," Regional Anesthesia and Pain Medicine, vol. 39, pp. 230–239, May-Jun 2014. [PubMed: 24705687]

[22]. Datta V, Mackay S, Mandalia M, and Darzi A, "The use of electromagnetic motion tracking analysis to objectively measure open surgical skill in the laboratory-based model," Journal of the American College of Surgeons, vol. 193, pp. 479–485, 11 2001. [PubMed: 11708503]

[23]. Moorthy K, Munz Y, Sarker SK, and Darzi A, "Objective assessment of technical skills in surgery," British Medical Journal, vol. 327, pp. 1032–1037, 11 1 2003. [PubMed: 14593041]

[24]. Howells NR, Brinsden MD, Gill RS, Carr AJ, and Rees JL, "Motion analysis: A validated method for showing skill levels in arthroscopy," Arthroscopy-the Journal of Arthroscopic and Related Surgery, vol. 24, pp. 335–342, 3 2008.

[25]. Corvetto MA, Fuentes C, Araneda A, Achurra P, Miranda P, Viviani P, and Altermatt FR, "Validation of the imperial college surgical assessment device for spinal anesthesia," Bmc Anesthesiology, vol. 17, 9 29 2017.

[26]. Strom P, Hedman L, Sarna L, Kjellin A, Wredmark T, and Fellander-Tsai L, "Early exposure to haptic feedback enhances performance in surgical simulator training: a prospective randomized crossover study in surgical residents," Surgical Endoscopy and Other Interventional Techniques, vol. 20, pp. 1383–1388, 9 2006. [PubMed: 16823652]

[27]. Wanzel KR, Ward M, and Reznick RK, "Teaching the surgical craft from selection to certification," Current Problems in Surgery, vol. 39, pp. 577–659, 6 2002.

[28]. Amini R, Kartchner JZ, Stolz LA, Biffar D, Hamilton AJ, and Adhikari S, "A novel and inexpensive ballistic gel phantom for ultrasound training," World Journal of Emergency Medicine, vol. 6, pp. 225–228, 2015. [PubMed: 26401186]

[29]. Howes TE, Lobo CA, Kelly FE, and Cook TM, "Rescuing the obese or burned airway: are conventional training manikins adequate? A simulation study," Br J Anaesth, vol. 114, pp. 136–42, 1 2015. [PubMed: 25296912]

[30]. Higgins WT, "A Comparison of Complementary and Kalman Filtering," IEEE Transactions on Aerospace and Electronic Systems, vol. AES-11, pp. 321–325, 1975.

[31]. Barnett AC, Lee YS, and Moore JZ, "Fracture Mechanics Model of Needle Cutting Tissue," Journal of Manufacturing Science and Engineering-Transactions of the Asme, vol. 138, 1 2016.

[32]. Pepley D, Yovanoff M, Mirkin K, Miller S, Han D, and Moore J, "Measurement of Syringe Needle Forces for a Haptic Robotic Training Device," in Design of Medical Devices Conference, Minneapolis, MN, 2017.

[33]. Okamura AM, Simone C, and O'Leary MD, "Force modeling for needle insertion into soft tissue," Ieee Transactions on Biomedical Engineering, vol. 51, pp. 1707–1716, 10 2004. [PubMed: 15490818]

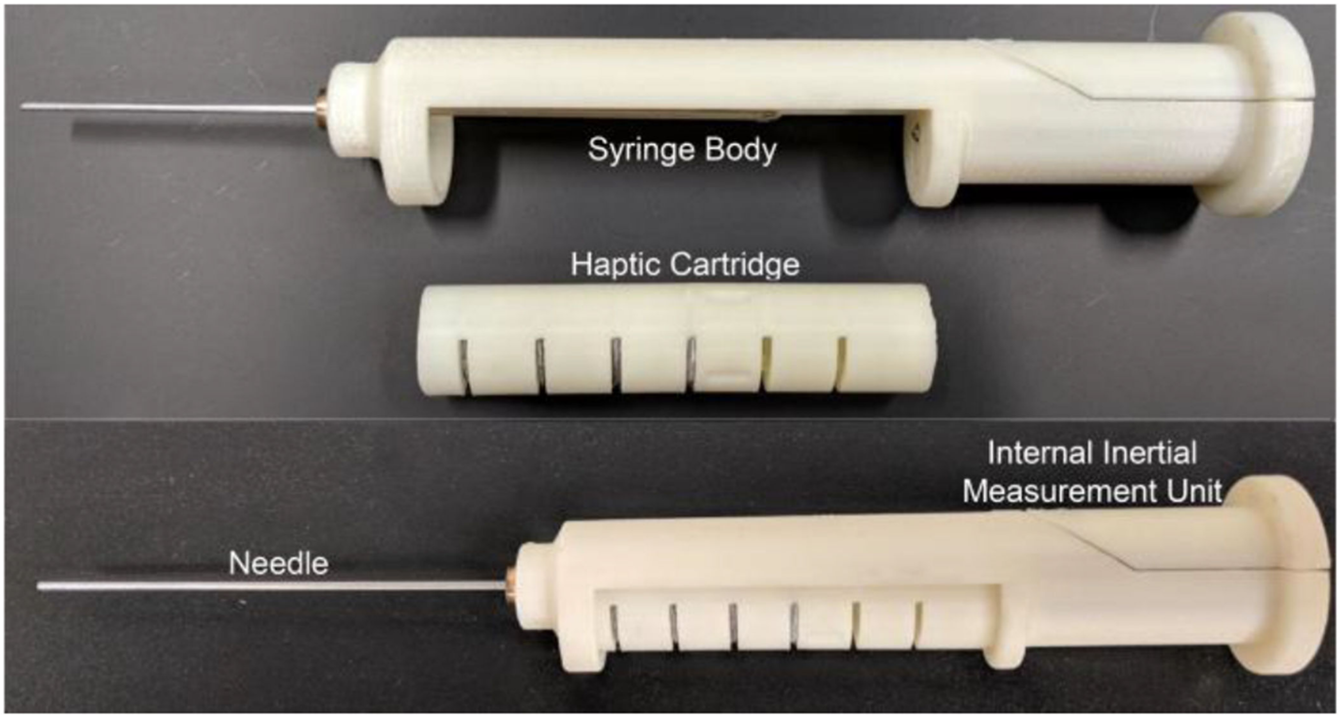

Fig. 1.

Pictured is the Low Cost Haptic Force Needle Insertion Simulator and one of the haptic cartridges used to provide force feedback.

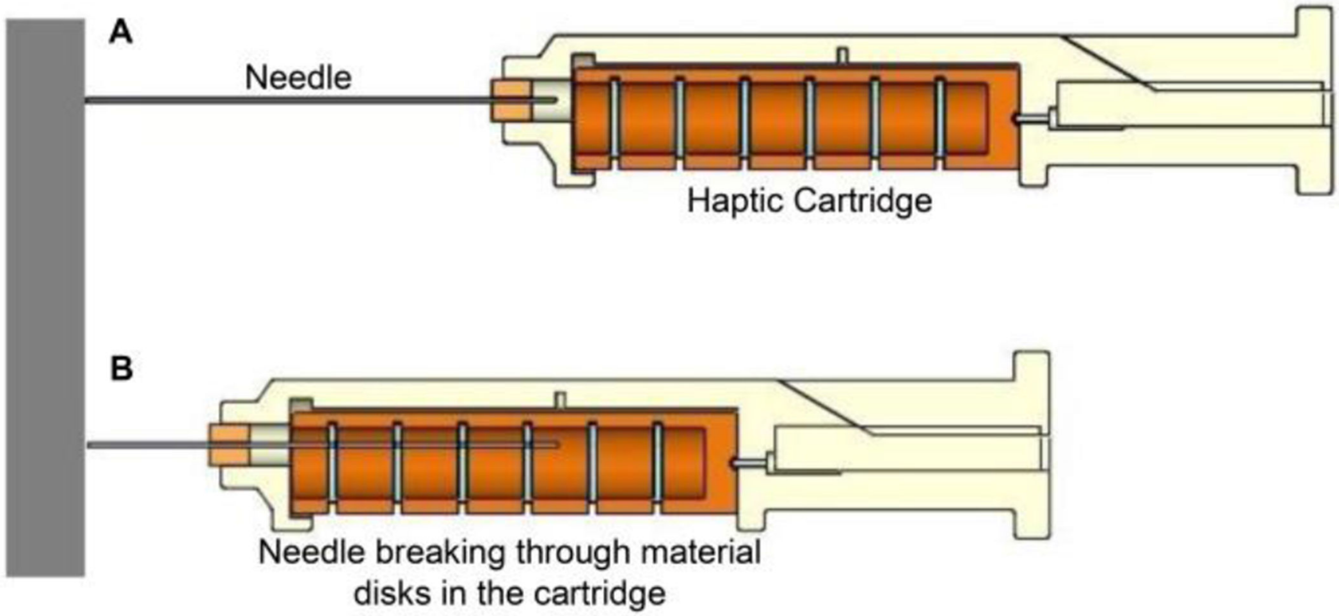

Fig. 2.
Cross-section view of the Low Cost Haptic Force Needle Insertion Simulator. (A) Needle Extended. (B) Insertion causes needle to slide into cartridge and break through disks of materials.

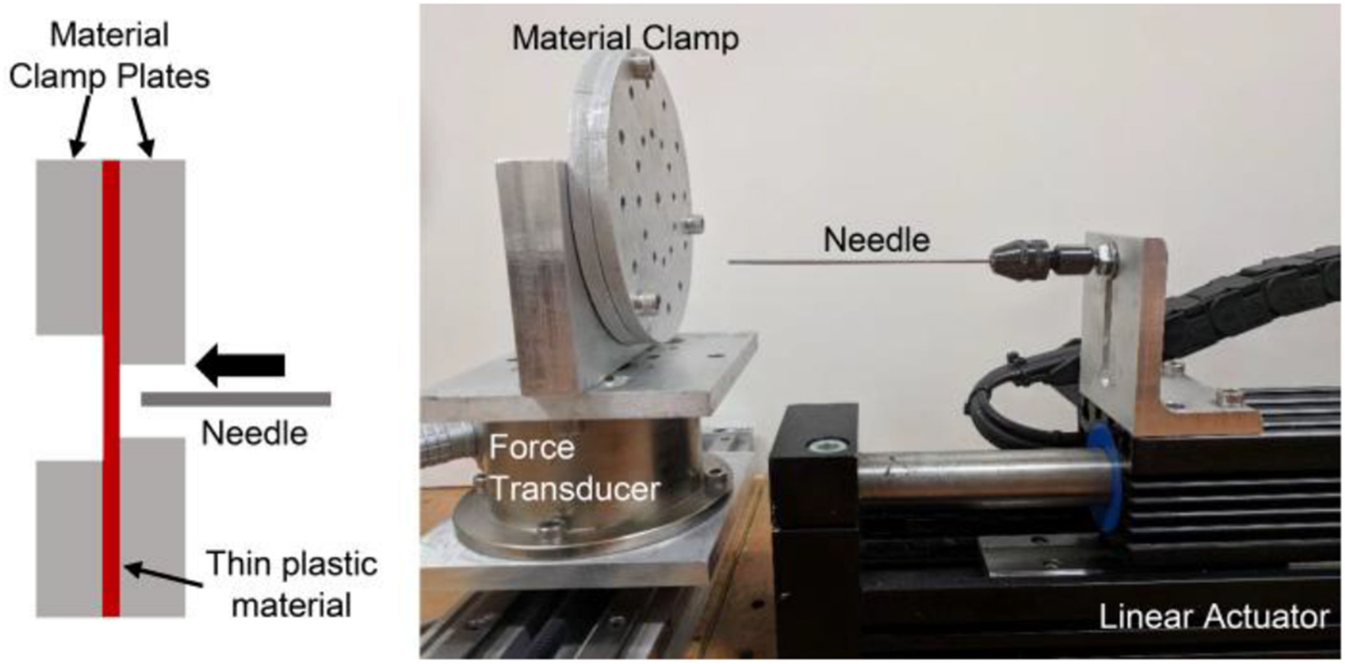

Fig. 3.
Experimental setup for needle insertions into thin plastic materials using a computer controlled linear actuator.

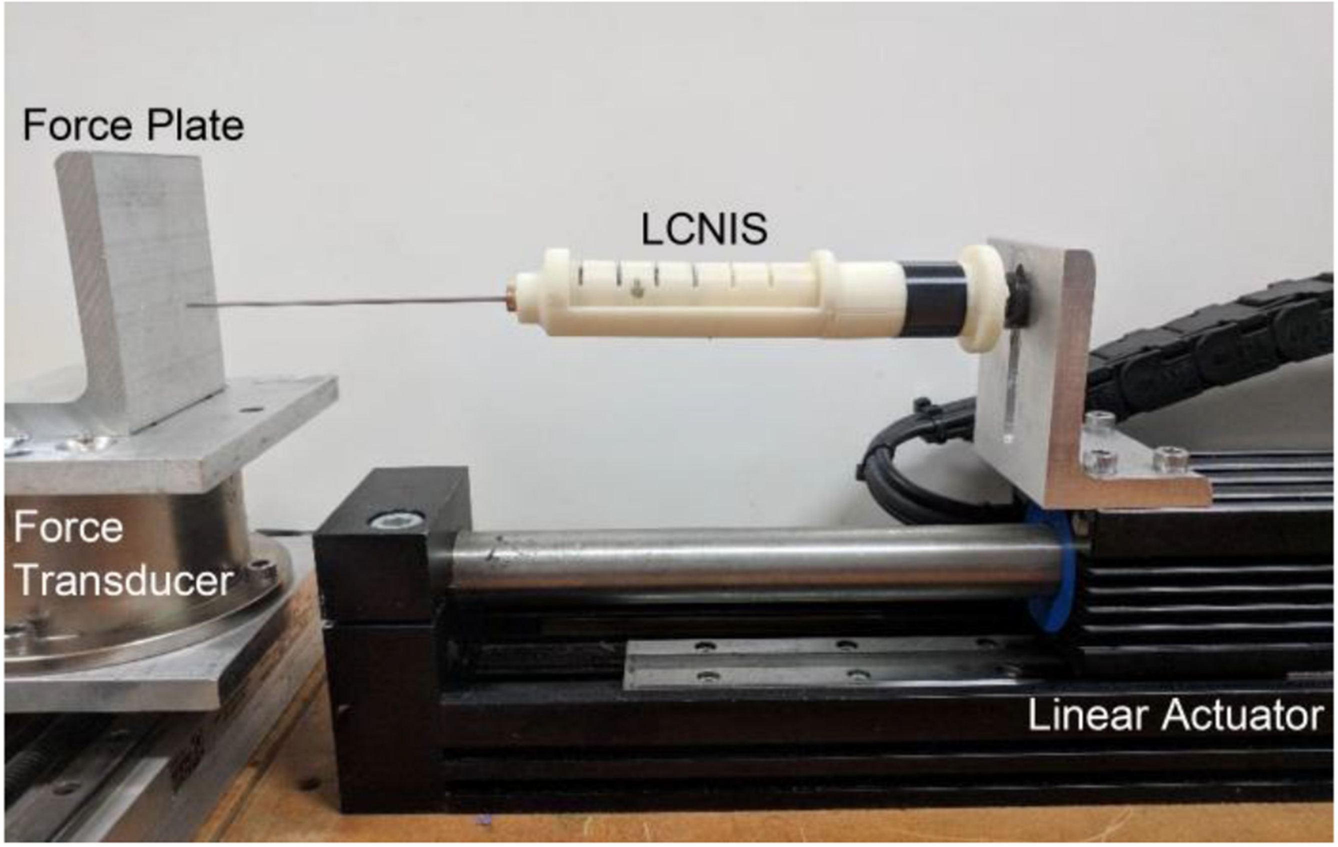

Fig. 4.

Experimental setup for measuring needle forces obtained from the Low Cost Haptic Needle Insertion Simulator (LCNIS).

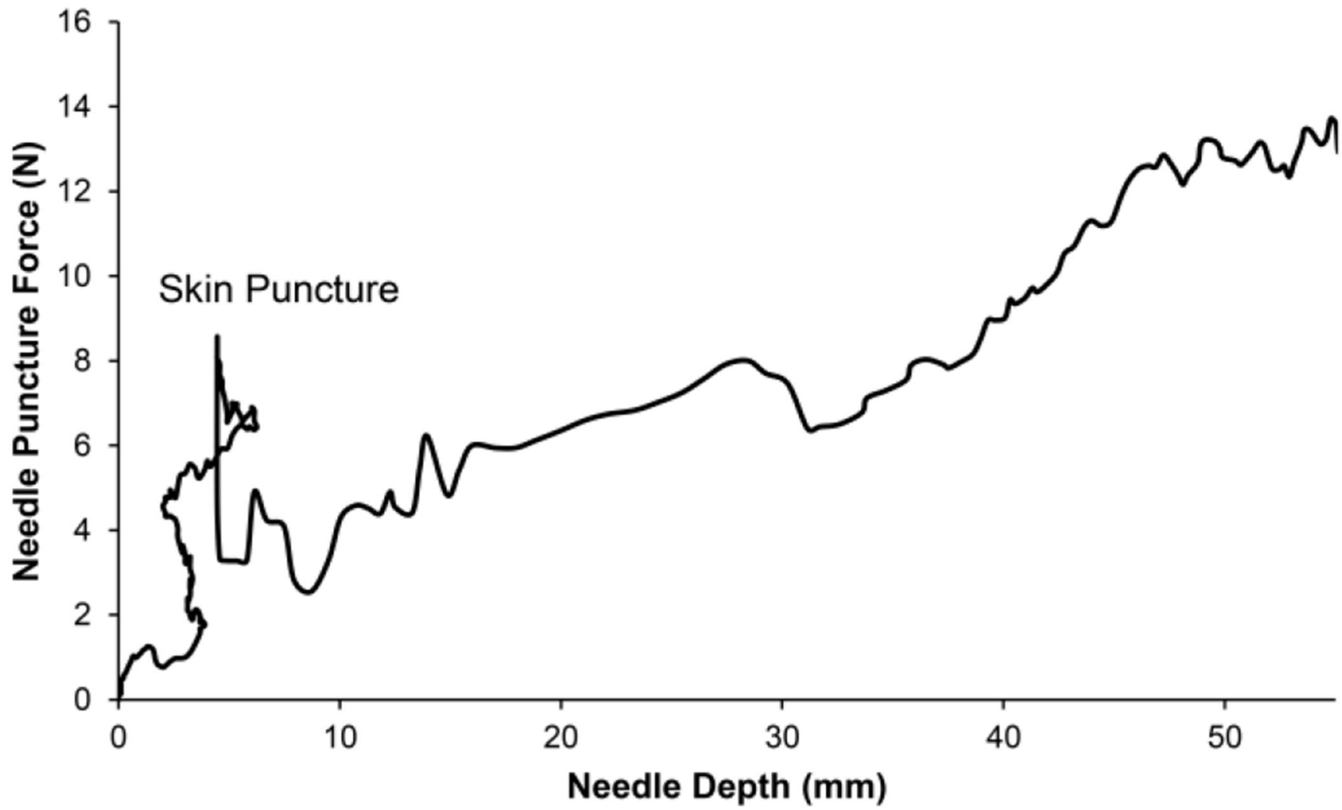

Fig. 5.
Measured needle forces versus needle depth during the insertion of a Pajunk SonoPlex Stim 21 Gauge 100 mm needle into the thigh of a cadaver.

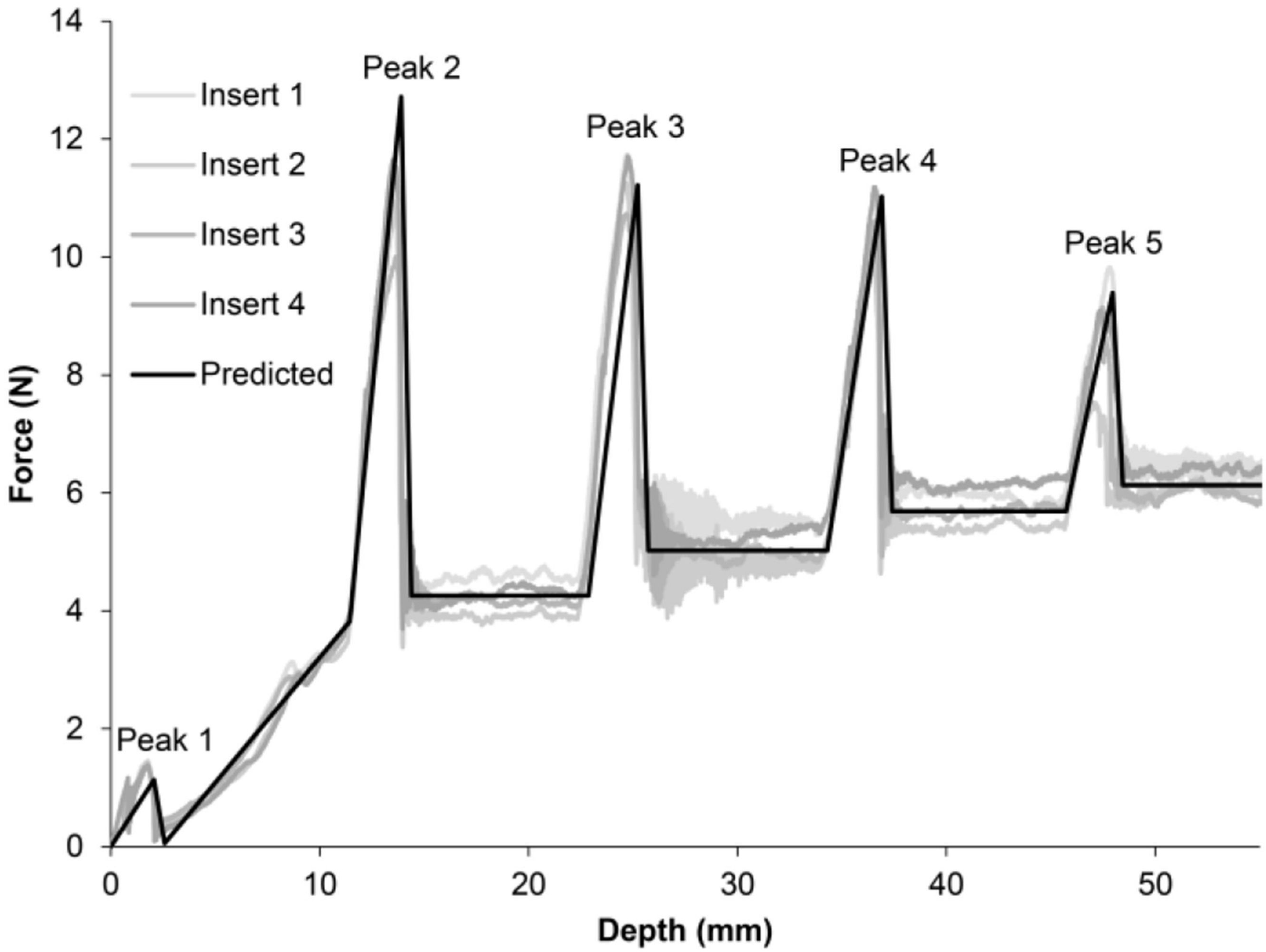

Fig. 6.

Needle forces from a haptic cartridge in the LCNIS containing a variety of thin plastic materials, and the predicted needle forces.

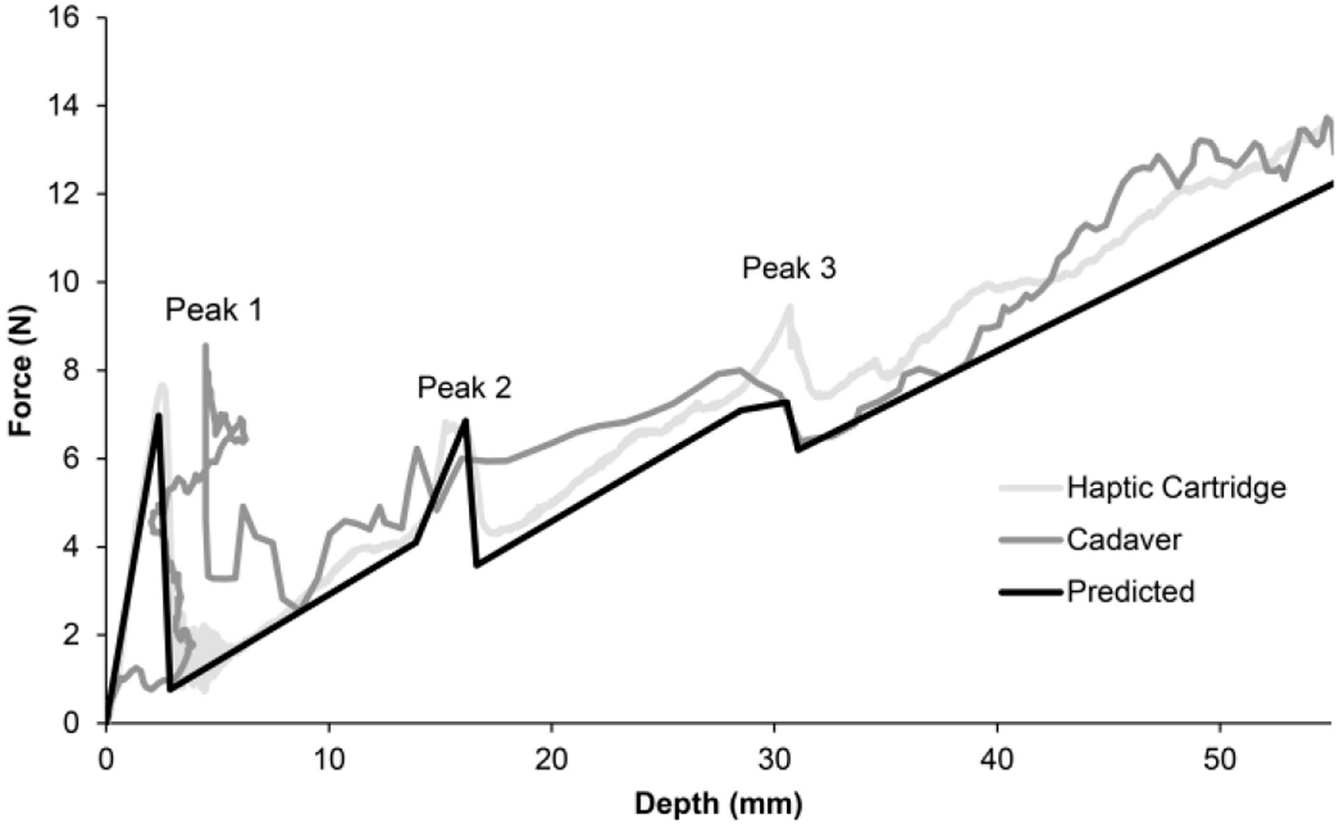

Fig. 7.

Needle forces from the custom cadaver haptic cartridge in the LCNIS and the predicted needle forces. Insertion 1 was removed due to significant measurement noise.

Fig. 8.
ABS plastic film disk used in LCNIS haptic cartridge. Four distinct puncture holes are shown from four insertions using the LCNIS.

Table 1.

Explanation of symbols used in Equations (1) and (2).

a_x	Acceleration in the X direction relative to the IMU sensor coordinate frame (m/s^2)
a_y	Acceleration in the Y direction relative to the IMU sensor coordinate frame (m/s^2)
a_z	Acceleration in the Z direction relative to the IMU sensor coordinate frame (m/s^2)
dt	Measurement time interval (s)
θ	Current needle angle relative to ground surface (deg)
θ_0	Previous needle angle relative to ground surface (deg)
θ_x	Needle angle derived from gravitational acceleration (deg)
ν	Angular velocity measured by gyroscope (deg)

Table 2.

List of four experiments conducted, the materials used in each test, and each testing apparatus.

Experiment	Purpose	Materials	Insertion Force Measurement Apparatus
1	Measure needle insertion forces into a cadaver thigh	Cadaver thigh tissue	Hand-held force sensing syringe with 6-axis force transducer
2	Determine material properties for use in the LCNIS haptic cartridge	PTFE, Polycarbonate, PVC, UHMW, ABS, FEP	Linear actuator with six axis force transducer
3	Create and validate LCNIS haptic cartridge force prediction equation	LCNIS haptic cartridge containing PTFE, Polycarbonate, PVC, UHMW, ABS	Linear actuator with six axis force transducer
4	Create LCNIS haptic cartridge mimicking a cadaver	LCNIS haptic cartridge containing PTFE, PVC, ABS	Linear actuator with six axis force transducer

Table 3.

Thickness and cartridge depth of the materials used in the haptic cartridge in Experiment 3.

Material	Thickness (mm)	Depth (mm)
PTFE	0.05	0
PVC	11.40	0.05
Polycarbonate	0.13	11.4
ABS	0.08	45.7
ABS	0.13	22.9
UHMW	0.10	34.3

Table 4.

Measured peak and friction forces for haptic cartridge materials from linear motor experiment.

Material	Peak Force (N)	Depth of Max Force (mm)	Friction Force (N)
PTFE	1.13	2.06	0.05
Polycarbonate	9.85	2.46	1.38
ABS 0.08 mm	3.70	2.24	0.44
ABS 0.13 mm	6.97	2.36	0.77
UHMW	6.00	2.61	0.67
FEP	0.84	2.19	0.11
PVC	= 0.2153 * Depth + .948	chosen	.948

Table 5.

Symbols used in haptic cartridge needle force prediction equation

x	Needle Depth
n	Number integer label for material, first material $n = 1$, second $n = 2$, …
Z_n	Depth of material n (mm)
D_n	Depth of maximum force for material n
F_{Pn}	Peak force of material n
f_n	Friction force of material n

Table 6.

Materials and locations of the materials used in the LCNIS custom cadaver haptic cartridge.

Material	Thickness (mm)	Depth (mm)
ABS	0.127	0
PVC	13.8	0.127
ABS	0.0762	13.9
PVC	14.5	14.0
PTFE	0.0508	28.5
PVC	29.3	28.6